

Preparation of char from lotus seed biomass and the exploration of its dye removal capacity through batch and column adsorption studies

S. Nethaji · A. Sivasamy · R. Vimal Kumar · A. B. Mandal

Received: 22 August 2012 / Accepted: 16 October 2012 / Published online: 7 November 2012
© Springer-Verlag Berlin Heidelberg 2012

Abstract Char was obtained from lotus seed biomass by a simple single-step acid treatment process. It was used as an adsorbent for the removal of malachite green dye (MG) from simulated dye bath effluent. The adsorbent was characterized for its surface morphology, surface functionalities, and zero point charge. Batch studies were carried out by varying the parameters such as initial aqueous pH, adsorbent dosage, adsorbent particle size, and initial adsorbate concentration. Langmuir and Freundlich isotherms were used to test the isotherm data and the Freundlich isotherm best fitted the data. Thermodynamic studies were carried out and the thermodynamic parameters such as ΔG , ΔH , and ΔS were evaluated. Adsorption kinetics was carried out and the data were tested with pseudofirst-order model, pseudosecond-order model, and intraparticle diffusion model. Adsorption of MG was not solely by intraparticle diffusion but film diffusion also played a major role. Continuous column experiments were also conducted using microcolumn and the spent adsorbent was regenerated using ethanol and was repeatedly used for three cycles in the column to determine the reusability of the regenerated adsorbent. The column data were modeled with the modeling equations such as Adam-Bohart model, Bed Depth Service Time (BDST) model, and Yoon-Nelson model for all the three cycles.

Keywords Char · Lotus seed · Isotherms · Kinetics · Thermodynamics · Column regeneration

Introduction

All the organic materials that have their origin from living things are termed as biomass. Therefore, the sources for biomass are diverse. Hence, biomass accounts for 14 % of the world's total energy supply to mankind (Gupta et al. 2011b). Wastes from biomass have to be disposed off with additional cost. Therefore, a proper treatment route to convert biomass waste to useful end product would offset the costs of treatment and disposal (Williams and Reed 2006). Adsorption by activated carbons prepared from biomass has been widely used for the industrial effluent treatment (Kaushik and Thakur 2012). Since activated carbons have extended surface area, complex porous structures, and high surface reactivity, it is being used as adsorbent for the removal of a wide range of pollutants dissolved in aqueous solutions (Wang et al. 2012). However, the regeneration and reuse of activated carbon results in steep decrease in its efficiency (Khenifi et al. 2007). Also, the commercially available carbon is not economically feasible for large scale owing to its high cost (Gupta and Ali 2008). Hence, low-cost adsorbents were investigated and the materials which have adsorption capacity in its natural state have been studied (Gupta et al. 2000). However, the adsorption capacity was found to be very low for the raw biomass when compared to the activated carbon derived from the biomass (Gupta et al. 2010; Jain et al. 2004). The possibility of using char from biomass as an adsorbent was less explored. Char can be prepared mainly by two methods, namely, thermal treatment and chemical treatment. Chemical treatment has two important advantages over thermal treatment. One is the lower process temperature and the other is the yield tends to

Responsible editor: Vinod Kumar Gupta

Electronic supplementary material The online version of this article (doi:10.1007/s11356-012-1267-4) contains supplementary material, which is available to authorized users.

S. Nethaji · A. Sivasamy (✉) · R. V. Kumar · A. B. Mandal
Chemical Engineering Area, CSIR-Central Leather Research
Institute (Council of Scientific & Industrial Research),
Adyar, Chennai 600 020, India
e-mail: arumugamsivasamy@yahoo.co.in

be greater due to the fact that burn-off char is not required. Chemical treatment has been carried out with dehydrating agents such as $ZnCl_2$ (Yalcin and Sevinc 2000), H_3PO_4 (Nakagawa et al. 2007), HCl (Alvarez et al. 2007), and H_2SO_4 (Gercel and Gercel 2007). Sulfuric acid is preferred since it's an inexpensive and nonvolatile chemical than other dehydrating agents such as $ZnCl_2$ due to the environmental contamination problems by zinc compounds (Guo et al. 2005). Therefore, in the present study, char was prepared from lotus seed (*Nelumbo nucifera*) biomass by a single-step sulfuric acid treatment process.

Wastes from industries are often discharged to the nearest water bodies such as lakes, rivers, and seas due to rapid technology development (Gupta et al. 2012a, b). The effluents of leather and textile industries are the major cause of environmental and drinking water pollution. The effluents from these industries are the source of pollutants like bases, acids, organics, inorganics, dissolved solids, and color. The presence of color is the most undesirable because it can be recognized easily (Gupta et al. 2006c, 2007a). Such colors are produced by dyes which are generally toxic, stable, and nondegradable (Gupta et al. 2007b). Approximately 40,000 dyes and pigments with over 7,000 different chemical structures have been identified (Pitter and Chudoba 1990). It was estimated that 7,00,000 t of dyes and pigments per year are produced globally (Gupta et al. 2011a, b, c, d). Ten to fifteen percent of the dye used for the dyeing process is lost in the effluent (Lian et al. 2009). Industrial wastewaters carry approximately 20 % of these discharged dyes (Essawy et al. 2008). Many techniques which include ion exchange, chemical reduction, electrochemical processes (Gupta et al. 2007d), advanced oxidation processes (Gupta et al. 2007c, 2011c, d, 2012a, b), biosorption (Gupta and Rastogi 2009), and membrane technology have been applied for the removal of dyes from industrial effluents. However, adsorption is inexpensive, fast, and can remove pollutants even at low concentrations (Gupta et al. 2007e; Mittal et al. 2005).

Malachite green (MG) is a basic and cationic dye which has been widely used. A report from animal studies suggested that since MG contained nitrogen atoms, it had carcinogenic, mutagenic, genotoxic, and teratogenic properties, thus affecting the biodegradability and removal of MG dye (Zang et al. 2008). In recent years, various adsorbents such as natural zeolite (Han et al. 2008), chitin hydrogels (Tang et al. 2012), rice husk (Chowdhury and Saha 2012), ginger waste (Ahmad and Kumar 2010), neem saw dust (Khattari and Singh 2009), coffee bean (Baek et al. 2010), and sea shell powder (Chowdhury and Saha 2010) were used for the adsorption of MG from aqueous solution. This study reports, for the first time, on the feasibility of applying char obtained from lotus seed biomass (CLS) as a low-cost alternative adsorbent for the adsorption of MG.

Materials

MG dye was received from SD Fine Chemicals, Mumbai, India. Sulfuric acid, sodium chloride, sodium hydroxide, sodium bicarbonate, HCl , and sodium carbonate were procured from Merck (India), Mumbai, India. *N. nucifera* seed (lotus seed biomass) was collected from the local market from Chennai, India. The biomass was then crushed into small pieces and the sand and dirt were removed by washing with distilled water followed by drying in sunlight for 2 days. The dried biomass was then acid treated with 1:1 ratio of concentrated H_2SO_4 :biomass for 48 h. The obtained char was neutralized by washing with water and dried in a hot air oven at 140 °C for 48 h. The dried lotus seed char (CLS) was powdered by ball milling and then separated by mechanical sieving to particle sizes of 100 μm , 600 μm , and 1,000 μm .

The prepared CLS was characterized for its zero point charge by powder addition method (Preethi and Sivasamy 2006), surface morphology by Scanning Electron Microscope (SEM) of Hitachi make and model S-3400 N, and surface acid functional group of CLS by Boehm titration (Boehm 1966). The MG stock solution was prepared by dissolving 1,000 mg of MG in 1 L of distilled water and the desired working solutions of different concentrations were prepared from the stock solution.

A double beam UV/visible spectrophotometer (Shimadzu UV-2102 PC) was employed to determine the unknown concentration of MG. The unknown dye concentrations were estimated by interpreting the absorbance with the standard calibration chart at (λ_{max}) 625 nm. The aqueous pH measurements were carried out in Digisun Electronics System (digital pH meter model 2001).

Amount of MG adsorbed at equilibrium was calculated by:

$$q_e = \frac{(c_0 - c_e)v}{w} \quad (1)$$

Amount of MG adsorbed at time t was calculated by:

$$q_t = \frac{(c_0 - c_t)v}{w} \quad (2)$$

where C_0 and C_e (milligrams per liter) are the liquid phase initial and equilibrium concentrations of the dye, respectively. C_t (milligrams per liter) is the liquid phase concentration of MG at time t . V is the volume of the solution (liters), and W is the mass of dry adsorbent used (grams). The equilibrium and kinetic experiments were duplicated and the experimental data and results were within 5 % error.

Results and discussion

Characterization of CLS

The prepared CLS was characterized by its surface acidity, zero-point charge, and SEM. The total surface acidity was

found to be $0.6135 \text{ meq g}^{-1}$ (phenolic groups $0.5073 \text{ meq g}^{-1}$, lactonic groups $0.0252 \text{ meq g}^{-1}$, carboxylic groups 0.081 meq g^{-1}). The zero-point charge (pH_{zpc}) of CLS was at pH 3. The SEM micrographs of CLS before and after adsorption were displayed in Fig 1.

Batch experiments

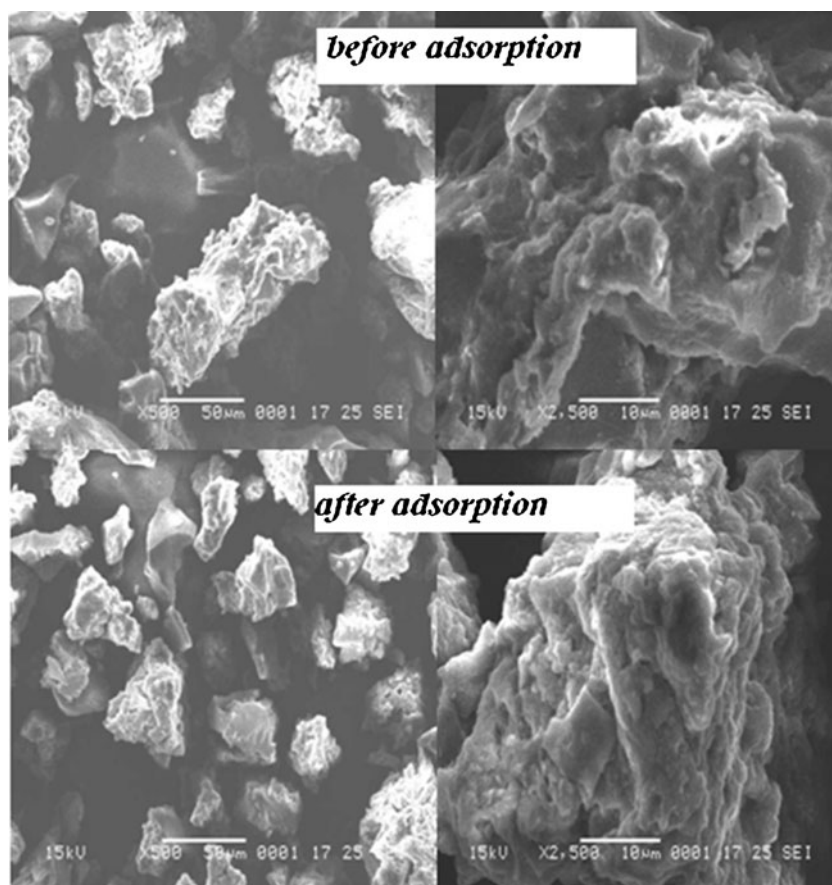
Batch experiments were carried out by studying the effect of initial pH, adsorbent dosage, particle size of the adsorbent, and initial dye concentration. The initial aqueous phase pH was varied from pH 2 to 10. The pH_{zpc} of the adsorbent played an important role in the effect of initial pH. The surface charge of CLS was positive when the solution pH was below pH_{zpc} and negative when it was above pH_{zpc} (Gupta and Sharma 2003). Since MG is a basic dye, it ionizes into positively charged ions in solution. The pH_{zpc} of CLS was at pH 3 and hence, the surface was negatively charged above pH 3 which corresponds to the maximum adsorption of MG at pH ranging from 6.0 to 9.0 (Fig. S1 in the supplementary material). Hence, distilled water was used for further experiments. The percent adsorption increased with the increase in the adsorbent dosage (Fig. S2 in the supplementary material) and decrease in the initial dye concentration. The optimum dosage was found to be 0.1 g/10 mL . The effect of particle size of the adsorbent

was studied by varying the particle sizes as $100 \mu\text{m}$, $600 \mu\text{m}$, and $1,000 \mu\text{m}$ and the graph was shown in Fig S4 in the supplementary material. It was found that percent adsorption increased with the decrease in the particle size of CLS and so $100\text{-}\mu\text{m}$ particle size of CLS was used for further experiments. It is because the surface area increases with the decrease in the particle sizes (Gupta et al. 2006a). Hence, percent adsorption increased with the increase in adsorbent dosage, decrease in dye concentration, and decrease in adsorbent particle size. This was because of the increase in the adsorbent dosage which leads to the increase in the adsorbent surface area which, in turn, increases the active sites on the surface of the adsorbent.

Equilibrium studies and adsorption isotherms

Equilibrium studies were carried out to determine the conditions for maximum MG removal onto CLS at 293 K, 300 K, and 313 K. The adsorption process reaches equilibrium, beyond which the adsorption of adsorbate onto the adsorbent slows down considerably. This adsorption equilibrium could be expressed by two well known isotherm models, namely, Langmuir and Freundlich adsorption isotherms. The former corresponds to the homogeneous monolayer adsorption, whereas the latter defines the adsorption onto the adsorbent

Fig. 1 SEM micrograph of CLS before and after adsorption



with heterogeneous surface. The linear form of Freundlich isotherm model is as follows (Freundlich 1906):

$$\log q_e = \log K_F + \frac{1}{n} \log C_e \tag{3}$$

where, q_e is the equilibrium dye concentration in the solid phase (milligrams per gram), C_e is the equilibrium dye concentration in the aqueous phase (milligrams per liter), K_F (liters per gram) is the Freundlich constant and n (grams per liter) is the Freundlich exponent. The plot for Freundlich isotherm was displayed in Fig. 2. The values for K_F and n for all the three temperatures are provided in Table 1. Since the value of constant n is between 1 and 10, it indicates a favorable adsorption.

The monolayer adsorption onto the homogeneous adsorbent surface was defined by Langmuir isotherm. The linear form of the Langmuir isotherm is (Langmuir 1918):

$$\frac{1}{q_e} = \frac{1}{q_m K_L C_e} + \frac{1}{q_m} \tag{4}$$

where K_L is the Langmuir equilibrium constant (milligrams per liter) and q_m is the maximum monolayer dye concentration in the solid phase (milligrams per gram). The nature of the adsorption process can be determined by the dimensionless equilibrium parameter which was determined by the following equation:

$$R_L = \frac{1}{1 + K_L C_0} \tag{5}$$

where C_0 is the initial dye concentration (milligrams per liter). The values of R_L (<1) indicates the favorable adsorption. Langmuir isotherm plot was displayed in Fig. 2. The values of q_m , K_L , and R_L for all the three temperatures were given in Table 1. The equilibrium data were well fitted with

both Langmuir and Freundlich isotherms, since the r^2 values of the isotherms were closer to unity. Also, the equilibrium studies revealed that the monolayer saturation capacity increased with the increase in temperature.

Adsorption kinetics

Kinetic studies were carried out for four different initial dye concentrations: 25 mgL⁻¹, 50 mgL⁻¹, 75 mgL⁻¹, and 100 mgL⁻¹. Initially, the adsorption was quick due to the presence of more active sites and it gradually slowed down as the time progressed. To determine the kinetics of adsorption of MG onto CLS, pseudofirst-order model, pseudosecond-order model, and intraparticle diffusion model were applied. The linear form of pseudofirst-order kinetic model is given by (Li et al. 2011):

$$\ln(q_e - q_t) = \ln q_e - k_1 t \tag{6}$$

where q_e (milligrams per gram) and q_t (milligrams per gram) are the amounts of adsorbed adsorbate at equilibrium and at time t , respectively, and k_1 (per minute) is the rate constant of pseudofirst-order adsorption. The pseudosecond-order model is expressed as (Gupta et al. 2011a):

$$\frac{t}{q_t} = \frac{1}{k_2 q_e^2} + \frac{1}{q_e} t \tag{7}$$

where, k_2 (grams per milligram per minute) is the equilibrium rate constant of pseudosecond-order adsorption. The plots for pseudofirst-order and pseudosecond-order equations were shown in Fig. S4 in the supplementary material and Fig. 3, respectively. The values of k_1 , k_2 , and q_e were calculated from the respective plots and given in Table 1. It can be seen that the values of the correlation factor for both pseudofirst-order and

Fig. 2 Freundlich and Langmuir isotherm for the adsorption of MG onto CLS (ads.dosage=0.1 g/10 mL; pH 6.84; T=300 K; t=24 h; agitation=100 rpm)

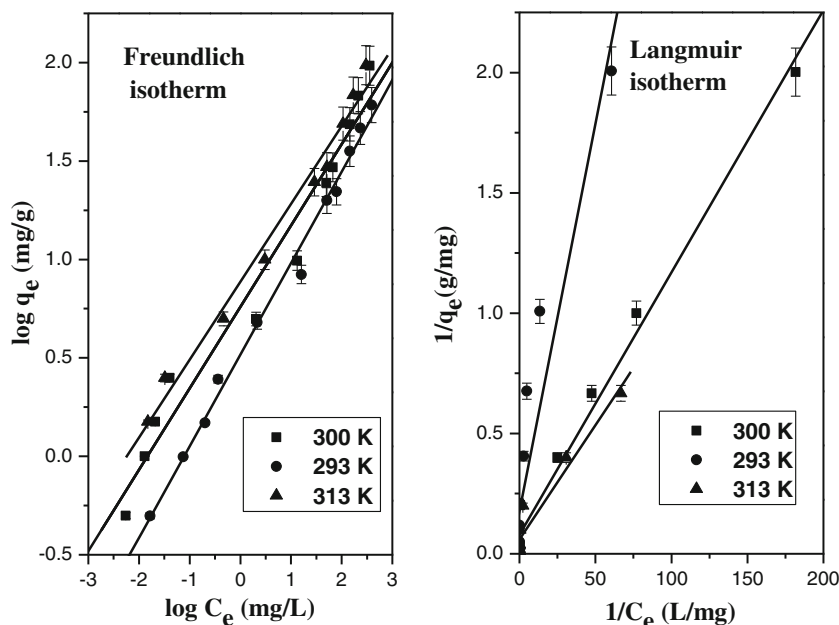


Table 1 Adsorption isotherm and kinetic model parameters for the adsorption of MG onto CLS

Adsorption isotherm					
Langmuir isotherm	Isotherm parameters	293 K	300 K	313 K	
	q_m (mg/g)	5.67	12.61	16.75	
	K_L	5.46	7.27	6.28	
	R_L	0.154–0.00018	0.120–0.00013	0.137–0.00015	
	r^2	0.94323	0.99383	0.9681	
	Standard deviation	0.21625	0.07238	0.06083	
Freundlich isotherm	K_f (L/g)	0.516	0.759	0.886	
	N	2.151	2.419	2.529	
	r^2	0.99607	0.98291	0.99218	
	Standard deviation	0.06756	0.15385	0.08639	
Temkin isotherm	B_1	4.984	5.90863	7.40	
	K_T (L/mg)	49.39	119.33	141.90	
	r^2	0.853	0.7963	0.8302	
	Standard deviation	11.479	20.537	19.919	
Adsorption kinetics					
Pseudofirst-order model	Kinetic parameters	25 mg/L	50 mg/L	75 mg/L	100 mg/L
	k_1 (L/min)	0.187	0.131	0.104	0.065
	q_e (mg/g)	1.958	4.481	8.255	5.824
	r^2	0.97666	0.96093	0.9481	0.98164
	Standard deviation	0.37666	0.50117	0.89114	0.49298
Pseudosecond-order model	k_2 (g/mgmin)	0.200	0.061	0.0345	0.0273
	q_e (mg/g)	2.440	4.785	6.934	9.000
	r^2	0.99974	0.99961	0.99925	0.99986
	Standard deviation	0.12271	0.11613	0.1788	0.08426
Intraparticle diffusion	K_i (mg/gmin ^{1/2})	0.145	0.264	0.284	0.296
	C	1.50241	2.7119	4.20891	5.80857

pseudosecond-order model were closer to unity. However, the experimental q_e values were very closer to the calculated q_e values for pseudosecond-order model which is not the

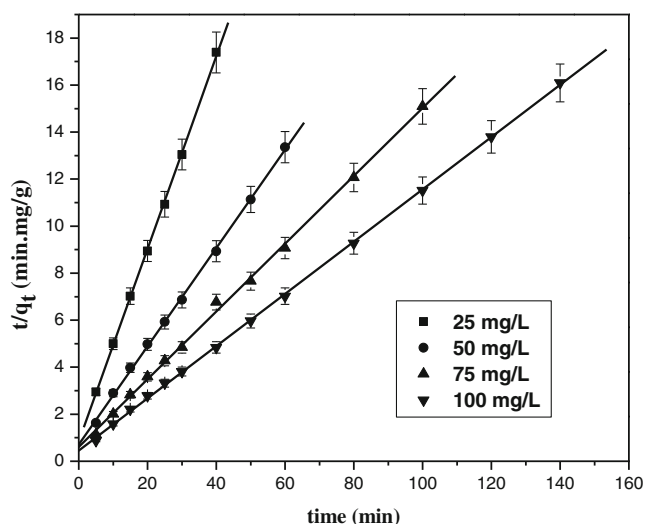


Fig. 3 Pseudosecond-order model for the adsorption of MG onto CLS (ads.dosage=1.5 g/150 mL; pH 6.84; $T=300$ K; agitation=150 rpm)

same in case of pseudofirst-order model. These results suggested that the pseudosecond-order model well described the adsorption of MG onto CLS. As shown in Table 1, the value of rate constant k_2 decreases with increasing initial MG concentration. Higher dye concentration corresponds to higher surface loadings which decreases the diffusion efficiency.

Intraparticle diffusion can be estimated by using the Weber–Morris intraparticle diffusion model (Zahoor and Mahramanlioglu 2011):

$$q_t = k_i t^{1/2} + c \quad (8)$$

where, q_t is the amount of solute on the surface of the sorbent at time t (milligrams per gram), k_i is the intraparticle diffusion rate constant (milligrams per gram per minute), and C is the intercept (milligrams per gram) and it corresponds to the thickness of the boundary layer. The values of k_i and C were evaluated from the plots shown in Fig. 4 and were tabulated in Table 1. If the intraparticle diffusion is involved in the adsorption process, then the Weber–Morris plot will be linear and if it is the rate-controlling step, then the plot will pass through origin. However, in the present study, the plot did not pass

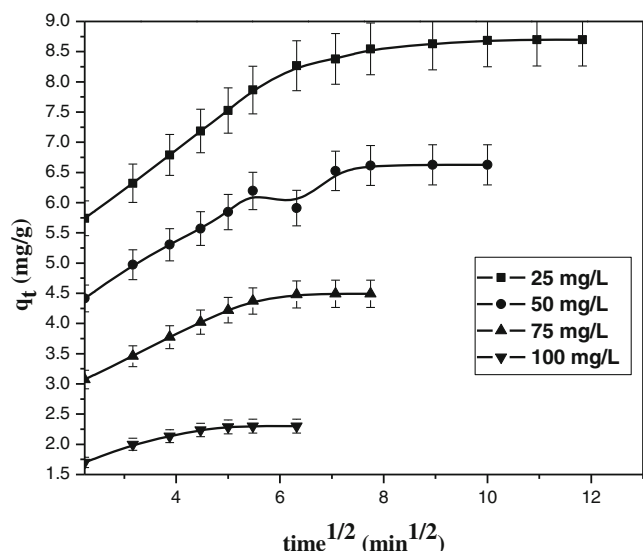


Fig. 4 Intraparticle diffusion model for the adsorption of MG onto CLS (ads.dosage=1.5 g/150 mL; pH 6.84; T=300 K; agitation=150 rpm)

through the origin, which indicates that intraparticle diffusion is not the only step involved in the adsorption process and boundary layer diffusion also takes place. An initial curve portion followed by a linear portion can be seen in Fig. 4. This initial curve portion represents the boundary layer diffusion while the later linear portion defines the intraparticle diffusion. Hence, the adsorption of MG onto CLS was by film diffusion followed by intraparticle diffusion. From Table 1, it is evident that the increase in MG concentration increased the thickness of the boundary layer.

Thermodynamic studies

The relation between the free energy of adsorption (ΔG) and Langmuir equilibrium constant can be expressed by the following expression (Gupta et al. 2006b):

$$\Delta G = -RT \ln K_L \tag{9}$$

Also, enthalpy changes (ΔH) and change in entropy (ΔS) in relation with the Langmuir equilibrium constant can be expressed as:

$$\ln K_L = \frac{\Delta S}{R} - \frac{\Delta H}{RT} \tag{10}$$

where R is the universal gas constant and T is temperature (Kelvin). The thermodynamic properties were calculated by plotting $\ln K_L$ versus $1/T$. The values of thermodynamic parameters were as follows: ΔG ($-4.0879 \text{ kJmol}^{-1}$, $-4.8889 \text{ kJmol}^{-1}$, and $-4.7245 \text{ kJmol}^{-1}$ for 293 K, 300 K, and 313 K, respectively), ΔH (3.739 kJmol^{-1}), and ΔS

($2.76 \text{ Jmol}^{-1} \text{K}^{-1}$). The negative values of ΔG indicated the spontaneity of the adsorption process. The positive value of ΔH indicated that the process was endothermic and the positive value of ΔS accounted for the increased randomness of adsorbate molecules on the solid surface than in the solution.

Column studies

To investigate the dynamic adsorption behavior, fixed-bed column experiments have been designed with glass columns of 1.2 cm inner diameter packed with 5 g of CLS, operated with influent dye concentration of 20 mgL^{-1} at a flow rate of 3 mLmin^{-1} . The total bed height was 5.5 cm and the corresponding bed volume was 6.22 cm^3 . The effluent samples were collected and analyzed for dye concentrations. After the saturation level was reached, the adsorbate was desorbed from the adsorbent by washing with ethanol and reused for the second and third cycles.

Analysis of column data

The packed bed column is analyzed through the concept of the breakthrough curve. The breakthrough curve for all the three cycles were shown in Fig. 5. The breakthrough point is the time at which the adsorbate species is detected in the column. This breakthrough point is the vital parameter in designing the large-scale adsorption columns. A breakthrough curve is usually defined as the ratio of effluent pollutant concentration to inlet pollutant concentration (C_t/C_0) as a function of flow time (t) or volume of effluent (V_{eff}) for a given bed height. The time at which

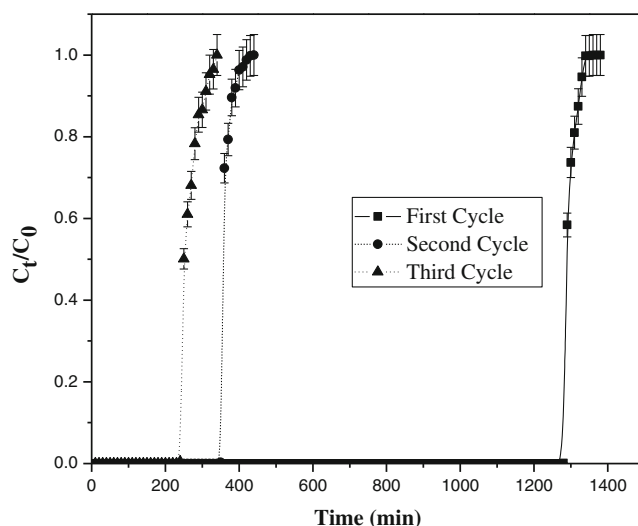


Fig. 5 Breakthrough curve for the adsorption of MG onto CLS (ads.dosage=5 g; [Dye]₀=20 mg/L; pH 6.84; T=300 K; bed height=5.5 cm; vol. flow rate=3 mL/min)

the adsorbate concentration in the effluent reached 1 mg/L is the breakthrough time (t_b) and the bed exhaustion time (t_e) is the time at which the dye concentration at the effluent reached 99.5 % of the initial dye concentration. Effluent volume (V_{eff}) was calculated as follows (Atar et al. 2011):

$$V_{eff} = F \cdot t_{total} \tag{11}$$

where F and t_{total} are volumetric flow rate and total flow time.

The total quantity of the adsorbate adsorbed in the column (m_{ad}) is represented by the area above the breakthrough curve multiplied by the flow rate. Total amount of the dye sent through the column (m_{total}) was calculated by the following equation:

$$m_{total} = C_o \cdot F \cdot t_e \tag{12}$$

Total dye removal percent of the column can be calculated from the following equation:

$$\text{Total removal (\%)} = \frac{m_{ad}}{m_{total}} \times 100 \tag{13}$$

The calculated column parameters such as t_b , t_e , m_{ad} , m_{total} , V_{eff} , and percent adsorption were tabulated in Table 2. It could be observed that the breakthrough time and the bed exhaustion time decreased considerably after the first cycle and thereby further decreasing the treated effluent volume and percent adsorption. However, the adsorption was in the range of 75 % even at the third cycle of operation attributing to the higher efficiency of regeneration of the spent adsorbent.

Modeling of column data

A number of mathematical models were developed for the use in design of column parameters. Among various models, three commonly used modeling equations such as Adams-Bohart model (Bohart and Adams 1920), Bed Depth Service Time (BDST) model (Han et al. 2008), and Yoon-Nelson model (Yoon and Nelson 1984) were used in modeling of the data obtained from the present study. They are as follows:

$$1. \text{ Adams – Bohart model : } \ln\left(\frac{C_t}{C_0}\right) = k_{AB}C_0t - k_{AB}N_0\left(\frac{Z}{v}\right) \tag{14}$$

$$2. \text{ BDST model : } t = \left(\frac{N_0Z}{C_0u}\right) - \left(\frac{1}{C_0k}\right) \ln\left(\frac{C_0}{C_t} - 1\right) \tag{15}$$

Table 2 Column parameters obtained at different cycles for the adsorption of MG onto CLS

Cycles	t_b (h)	t_e (h)	m_{ad} (mg)	m_{total} (mg)	v_{eff} (L)	% adsorption	Adams-Bohart model			BDST model			Yoon-Nelson model					
							$k_{AB} * 10^{-4}$ (Lmg ⁻¹ min ⁻¹)	N_0 (mgL ⁻¹)	r^2	Standard deviation	$k * 10^{-3}$ (Lmg ⁻¹ min ⁻¹)	r^2	Standard deviation	$k_{YN} * 10^{-2}$ (min ⁻¹)	τ (min)	r^2	Standard deviation	
I	21.3	22.6	77.73	81.36	4.07	95.53	4.23	780.77	0.9427	0.07096	6.08	15084.1	0.9825	0.05832	10.4	1292.4	0.8953	1.9419
II	6	7.33	21.76	26.38	1.31	82.48	4.02	565.96	0.9163	0.05014	3.57	4102.51	0.9723	0.06923	6.75	350.08	0.9721	1.8228
III	4	5.66	15.82	20.37	1.01	77.64	3.87	187.87	0.9439	0.07921	1.73	2772.82	0.9711	0.06972	4.09	250.06	0.9954	1.8311

$$3. \text{ Yoon – Nelson model : } \ln \frac{C_t}{C_0 - C_t} = k_{YN}t - \tau k_{YN} \quad (16)$$

where k_{AB} is the kinetic constant (liters per milligram per minute), N_0 is the maximum volumetric sorption capacity (milligrams per liter), v is the linear flow rate (centimeters per minute), Z is the bed height in the column (centimeters), k is the adsorption rate constant (liters per milligram per minute), u is the linear velocity (centimetres per minute), k_{YN} is the kinetic constant (per minute), and τ (minute) is the time required for retaining 50 % of the initial adsorbate concentration.

The plots for Adams-Bohart model, BDST model, and Yoon-Nelson model for all the three cycles were shown in Figs. S5, S6, and S7 in the supplementary materials, respectively. The parameters obtained from all the three modeling equations were tabulated in Table 2. From this table, it was evident that the constants of all the three modeling equations decreased with the number of cycles. Also, the volumetric adsorption capacity was considerably higher for the first cycle when compared to the consecutive cycles. While considering the correlation coefficient values, it could be well said that BDST model well fitted the column data.

Conclusion

CLS was found to be an efficient adsorbent for the adsorption of MG. Zero point charge was found to occur at pH 3.0 and thus, the percent adsorption was maximum at pH ranging from 6.0 to 9.0. Decrease in particle size increased the percent adsorption. Separation factor R_L of the Langmuir isotherm and n of the Freundlich isotherm confirmed that the studied adsorption process was favorable. Also, the adsorption of MG onto CLS followed both Langmuir and Freundlich isotherm models. Adsorption of MG onto CLS followed pseudosecond-order kinetic model. Thermodynamic parameters such as ΔG , ΔH , and ΔS were evaluated. Thermodynamic properties indicated that the adsorption process was spontaneous and endothermic. Continuous column studies were carried out and the adsorbent was regenerated using ethanol and used for three consecutive cycles. Efficiency of the adsorbent decreased to 95 %, 82 %, and 77 % for cycles I, II, and III, respectively. Continuous column data were interpreted with models, namely, Adams-Bohart model, BDST model, and Yoon-Nelson model and it was found that BDST model fitted the data well. Hence, it could be concluded that CLS was an effective adsorbent for the adsorption of MG and it was efficient enough even for the third cycle of operation.

Acknowledgments One of the authors (S.N.) would like to thank the Council for Scientific and Industrial Research (CSIR), New Delhi, India for providing financial support in the form of Research Fellowship to carry out this work.

References

- Ahmad R, Kumar R (2010) Adsorption studies of hazardous malachite green onto treated ginger waste. *J Environ Manage* 91:1032–1038
- Alvarez P, Blanco C, Granda M (2007) The adsorption of chromium (VI) from industrial wastewater by acid and base-activated lignocellulosic residues. *J Hazard Mater* 144:400–405
- Atar N, Olgun A, Wang S, Liu S (2011) Adsorption of anionic dyes on boron industry waste in single and binary solutions using batch and fixed-bed systems. *J Chem Eng Data* 56:508–516
- Baek MH, Ijagbemi CO, Jin OS, Kim DS (2010) Removal of Malachite Green from aqueous solution using degreased coffee bean. *J Hazard Mater* 176:820–828
- Boehm HP (1966) Chemical identification of surface groups. *Adv Catal* 16:179–274
- Bohart GS, Adams EQ (1920) Behavior of charcoal towards chlorine. *J Chem Soc* 42:523–529
- Chowdhury S, Saha PD (2010) Sea shell powder as a new adsorbent to remove Basic Green 4 (Malachite Green) from aqueous solutions: Equilibrium, kinetic and thermodynamic studies. *Chem Eng J* 164:168–177
- Chowdhury S, Saha PD (2012) Scale-up of a dye adsorption process using chemically modified rice husk: optimization using response surface methodology. *Desalin Water Treat* 37:331–336
- Essawy AA, El-Hag Ali A, Abdel-Mottaleb MSA (2008) Application of novel copolymer-TiO₂ membranes for some textile dyes adsorptive removal from aqueous solution and photocatalytic decolorization. *J Hazard Mater* 157:547–552
- Freundlich HMF (1906) Over the adsorption in solution. *J Phys Chem* 57:385–470
- Gercel O, Gercel HF (2007) Adsorption of lead (II) ions from aqueous solutions by activated carbon from biomass plant material of *Euphorbia rigida*. *Chem Eng J* 132:289–297
- Guo J, Xu WS, Chen YL, Lua AC (2005) Adsorption of NH₃ onto activated carbon prepared from palm shells impregnated with H₂SO₄. *J Colloid Interface Sci* 281(2):285–290
- Gupta VK, Ali I (2008) Removal of endosulfan and methoxychlor from water on carbon slurry. *Environ Sci Technol* 42:766–770
- Gupta VK, Rastogi A (2009) Biosorption of hexavalent chromium by raw and acid-treated green alga *Oedogonium hatei* from aqueous solutions. *J Hazard Mater* 163:396–402
- Gupta VK, Sharma S (2003) Removal of zinc from aqueous solutions using bagasse fly ash—a low cost adsorbent. *Ind Eng Chem Res* 42:6619–6624
- Gupta VK, Srivastava SK, Tyagi R (2000) Design parameters for the treatment of phenolic wastes by carbon columns (obtained from fertilizer waste material). *Water Res* 34(5):1543–1550
- Gupta VK, Mittal A, Gajbe V, Mittal J (2006a) Removal and recovery of the hazardous azo dye acid orange 7 through adsorption over waste materials: bottom ash and de-oiled soya. *Ind Eng Chem Res* 45:1446–1453
- Gupta VK, Mittal A, Krishnan L, Mittal J (2006b) Adsorption treatment and recovery of the hazardous dye, brilliant blue FCF, over bottom ash and de-oiled soya. *J Colloid Interface Sci* 293:16–26
- Gupta VK, Mittal A, Kurup L, Mittal J (2006c) Adsorption of a hazardous dye, erythrosine, over hen feathers. *J Colloid Interface Sci* 304:52–57
- Gupta VK, Ali I, Saini VK (2007a) Adsorption studies on the removal of vertigo blue 49 and orange DNA13 from aqueous solutions using carbon slurry developed from a waste material. *J Colloid Interface Sci* 315:87–93
- Gupta VK, Ali I, Saini VK (2007b) Defluoridation of wastewaters using waste carbon slurry. *Water Res* 41:3307–3316

- Gupta VK, Jain R, Mittal A, Mathur M, Sikarwar S (2007c) Photochemical degradation of the hazardous dye safranin-T using TiO₂ catalyst. *J Colloid Interface Sci* 309:464–469
- Gupta VK, Jain R, Varshney S (2007d) Electrochemical removal of the hazardous dye reactofix Red 3 BFN from industrial effluents. *J Colloid Interface Sci* 312:292–296
- Gupta VK, Jain R, Varshney S (2007e) Removal of reactor fix golden yellow 3 RFN from aqueous solution using wheat husk—an agricultural waste. *J Hazard Mater* 142:443–448
- Gupta VK, Rastogi A, Nayak A (2010) Adsorption studies on the removal of hexavalent chromium from aqueous solution using a low cost fertilizer industry waste material. *J Colloid Interface Sci* 342:135–141
- Gupta VK, Gupta B, Rastogi A, Agarwal S, Nayak A (2011a) A comparative investigation on adsorption performances of mesoporous activated carbon prepared from waste rubber tire and activated carbon for a hazardous azo dye-Acid Blue 113. *J Hazard Mater* 186:891–901
- Gupta VK, Gupta B, Rastogi A, Agarwal S, Nayak A (2011b) Pesticides removal from waste water by activated carbon prepared from waste rubber tire. *Water Res* 45:4047–4055
- Gupta VK, Jain R, Agarwal S, Shrivastava M (2011c) Kinetics of photo-catalytic degradation of hazardous dye Tropaeoline 000 using UV/TiO₂ in a UV reactor. *Colloids Surf A* 378:22–26
- Gupta VK, Jain R, Nayak A, Agarwal S, Shrivastava M (2011d) Removal of the hazardous dye—tartrazine by photodegradation on titanium dioxide surface. *Mater Sci Eng C* 31:1062–1067
- Gupta VK, Jain R, Agarwal S, Nayak A, Shrivastava M (2012a) Photodegradation of hazardous dye quinoline yellow catalyzed by TiO₂. *J Colloid Interface Sci* 366:135–140
- Gupta VK, Jain R, Mittal A, Saleh TA, Nayak A, Agarwal S, Sikarwar S (2012b) Photo-catalytic degradation of toxic dye amaranth on TiO₂/UV in aqueous suspensions. *Mater Sci Eng C* 32:12–17
- Han R, Dinf D, Xu Y, Zou W, Wang Y, Li Y, Zou L (2008) Use of rice husk for the adsorption of congo red from aqueous solution in column mode. *Bioresour Technol* 99:2938–2946
- Jain AK, Gupta VK, Jain S (2004) Suhas, Removal of chlorophenols using industrial wastes. *Environ Sci Technol* 38:1195–1200
- Khattari SD, Singh MK (2009) Removal of malachite green from dye wastewater using neem sawdust by adsorption. *J Hazard Mater* 167:1089–1094
- Khaushik G, Thakur IS (2012) Adsorption of colored pollutants from distillery spent wash by native and treated fungus: *Neurospora intermedia*. *Environ Sci Pollut Res*. doi:10.1007/s11356-012-0957-2
- Khenifi A, Bouberka Z, Sekrane F, Kameche M, Derriche Z (2007) Adsorption study of an industrial dye by organic clay. *Adsorption* 13:149–158
- Langmuir I (1918) The adsorption of gases on plane surface of glass, mica and platinum. *J Am Chem Soc* 40:1361–1403
- Li X, Zhou X, Mu J, Lu L, Han D, Lu C, Wang M (2011) Thermodynamics and kinetics of p-aminophenol adsorption on poly(aryl ether ketone) containing pendant carboxyl groups. *J Chem Eng Data* 56:4274–4277
- Lian L, Guo L, Guo C (2009) Adsorption of congo red from aqueous solutions onto Ca-bentonite. *J Hazard Mater* 161:126–131
- Mittal A, Krishnan L, Gupta VK (2005) Use of waste materials—bottom ash and de-oiled soya, as potential adsorbents for the removal of amaranth from aqueous solutions. *J Hazard Mater B* 117:171–178
- Nakagawa Y, Molina-Sabio M, Rodriguez-Reinoso F (2007) Modification of the porous structure along the preparation of activated carbon monoliths with H₃PO₄ and ZnCl₂. *Microporous Mesoporous Mater* 103:29–34
- Pitter P, Chudoba J (1990) Biodegradability of organic substances in the aquatic environment. CRC, Boca Raton
- Preethi S, Sivasury A (2006) Removal of safranin basic dye from aqueous solutions by adsorption onto corncob char. *Ind Eng Chem Res* 45:7627–7632
- Tang H, Zhou WJ, Zhang LN (2012) Adsorption isotherms and kinetic studies of malachite green on chitin hydrogels. *J Hazard Mater* 209–210:218–225
- Wang Z, Nie E, Li J, Yang M, Zhao Y, Luo X, Zheng Z (2012) Equilibrium and kinetics of adsorption of phosphate onto iron-doped activated carbon. *Environ Sci Pollut Res* 19:2908–2917
- Williams PT, Reed AR (2006) Development of activated carbon pore structure via physical and chemical activation of biomass fibre waste. *Biomass Bioenergy* 30:144–152
- Yalcin N, Sevinc V (2000) Studies of the surface area and porosity of activated carbons prepared from rice husks. *Carbon* 38:1943–1945
- Yoon Y, Nelson J (1984) Application of gas adsorption kinetics I. A theoretical model for respirator cartridge service time. *Am Ind Hyg Assoc J* 45:509–516
- Zahoor M, Mahramanlioglu M (2011) Adsorption of imidacloprid on powdered char and magnetic char. *Chem Biochem Eng Q* 25:55–63
- Zang J, Li Y, Zhang C, Jing Y (2008) Adsorption of malachite green from aqueous solution onto carbon prepared from arundo donax root. *J Hazard Mater* 150:774–782